[^{13}N]Ammonia

[^{13}N]NH_3

Kenneth T. Cheng, PhD[1]

Created: December 5, 2005; Updated: December 4, 2007.

Chemical name:	[^{13}N]Ammonia
Abbreviated name:	[^{13}N]NH_3
Synonym:	Ammonia N-13
Agent Category:	Compound
Target:	Glutamine synthetase
Target Category:	Metabolic trapping in cells by enzymatic conversion to [^{13}N]glutamic acid
Method of detection:	Positron Emission Tomography (PET)
Source of signal:	^{13}N
Activation:	No
Studies:	• *In vitro* • Rodents • Non-primate non-rodent mammals • Non-human primates • Humans

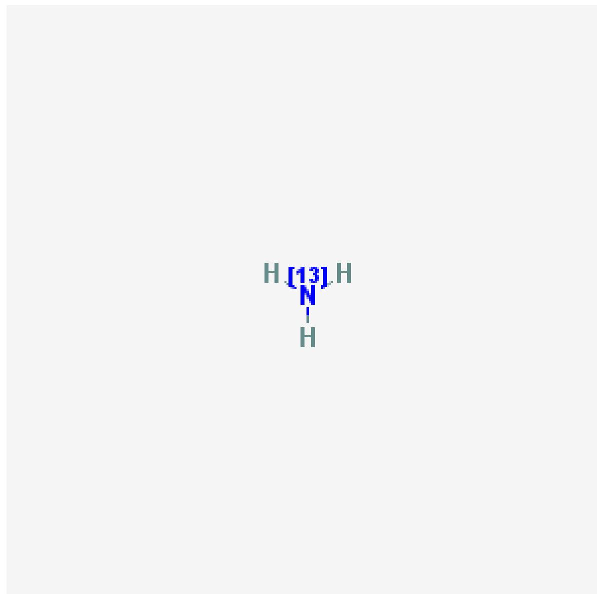

Click on the above structure for additional information in PubChem.

1 National Center for Biotechnology Information, NLM, NIH, Bethesda, MD; Email: micad@ncbi.nlm.nih.gov.

Background

[PubMed]

[^{13}N]Ammonia ([^{13}N]NH_3) is a useful ^{13}N-labeled compound that has been developed as a positron emission tomography (PET) imaging agent for assessing regional blood flow in tissues (1-3). The compound is labeled with ^{13}N which is a positron emitter with a physical $t_{½}$ of 9.965 min. [^{13}N]NH_3 was approved by the United States Food and Drug Administration in 2000 for PET imaging of the myocardium under rest or pharmacologic stress conditions to evaluate myocardial perfusion in patients with suspected or existing coronary artery disease.

Ammonia is important in many metabolic activities of various organs and is involved in biochemical pathways leading to the production of amino acids, purines, and urea (4). Ammonia is produced in the body from the deamination of amino acids and the deamidation of amides (5). About 20% of urea produced in the body is converted to ammonia and carbon dioxide in the gut. Ammonia is absorbed and converted back to urea in the liver. It also plays a significant role in glutamine synthesis. Ammonia is produced from glutamine and other amino acids in the kidney. NH_3, as a nonionic form, is freely permeable to all cell membranes (6). In an acidic environment, NH_3 accepts a proton and exists as NH_4^+. With a dissociation constant (pK_a) of 9.3, NH_4^+ constitutes about 99% of the total ammonia (NH_3 + NH_4^+) concentration in the pH range of body fluids. As an ionized form, NH_4^+ is a relatively impermeable cation to cell membranes. The mechanism of cellular localization of [^{13}N]NH_3 is not entirely known. One known mechanism is cellular membrane diffusion of [^{13}N]NH_3 and then metabolic trapping of radioactivity with the conversion of ammonia to glutamine, glutamic acid and carbamyl phosphate (6-8).

Ammonia labeled with ^{13}N was first produced by Joliot and Curie (9, 10). The short $t_{½}$ of ^{13}N requires on-site cyclotron production of ^{13}N and a short synthesis time of [^{13}N]NH_3. After i.v. intravenous injection, [^{13}N]NH_3 rapidly clears from the circulation. It is taken up mainly by the myocardium, brain, liver, kidneys, and skeletal muscle (2, 6, 11, 12). In the myocardium and brain, [^{13}N]NH_3 is removed from the blood and metabolically trapped within the tissues. The apparent linear relationship between distribution of [^{13}N]NH_3 and the regional blood perfusion makes feasible the use of this radiotracer for imaging and measuring cerebral and myocardial blood flows.

NLM Citation: Cheng KT. [^{13}N]Ammonia. 2005 Dec 5 [Updated 2007 Dec 4]. In: Molecular Imaging and Contrast Agent Database (MICAD) [Internet]. Bethesda (MD): National Center for Biotechnology Information (US); 2004-2013.

Synthesis

[PubMed]

As early as 1934, Joliot and Curie (10) first produced [^{13}N]NH_3 by alpha particle irradiation and heating of boron nitride in sodium hydroxide. Later, [^{13}N]NH_3 was produced by deuteron irradiation of methane gas or metal carbides, which gave relatively low yields (4). A more efficient method is the proton irradiation of a natural water target [^{16}O(p,α)^{13}N] (1, 13). In this procedure, [^{13}N]NH_3 is initially produced by hydrogen abstraction from the target water matrix. There is increasing production of oxo anions of nitrogen ($^{13}NO_3$– and $^{13}NO_2$–) from radiolytic oxidation with increasing target dose. These oxo anions can be converted to [^{13}N]NH_3 in aqueous solution by use of reducing reagents such as DeVarda's alloy in sodium hydroxide or titanium(III) chloride/hydroxide. Ido et al. (14) first described a fully automated synthesis method with titanium(III) chloride used as the reducing agent. The radiochemical purity was >99.9% and the radiochemical yield was 87-91% within 10 min from the end of bombardment (EOB). [^{13}N]NH_3 also can be produced directly in the target water (in-target production) by adding free radical scavengers (ethanol, acetic acid, or hydrogen) to prevent the formation of the oxo anions. Wieland et al. (15) applied this method for [^{13}N]NH_3 production with the use of pressurized, dilute aqueous solutions of acetic acid and ethanol. Berridge et al. (16) reported that the combination of hydrogen and ethanol was more effective than either alone at high beam doses. One limiting factor of the [^{16}O(p,α)^{13}N] nuclear reaction is that the relatively small cross-section of the reaction requires accelerators/cyclotrons of energies >10 MeV for production.

Ferrieri et al. (17) introduced a novel solid ^{13}C-enriched target for on-line [^{13}N]NH_3 production with use of the ^{13}C(p,n)^{13}N reaction. This nuclear reaction has a higher cross-section which can be used in accelerators/cyclotrons with <10 MeV energies. In their method, [^{13}N]nitrogen gas was converted to [^{13}N]NH_3 by use of microwave radiation to dissociate the nitrogen gas in a hydrogen plasma. The reaction time was about 10 min, and radiochemical yield was 25% at 10 min after the EOB. Bida et al. (18) also used the method of ^{13}C(p,n)^{13}N reaction by placing enriched ^{13}C carbon powder between two frits and irradiating with a 10 MeV proton beam while water was pumped through the bed to extract the ammonia. Welch et al. (19) successfully produced [^{13}N]NH_3 with the use of ^{12}C(d,n)^{13}N reaction and a 7 MeV deuteron beam in aluminum carbide. Shefer et al. (20) and Dence et al. (21) showed that a windowless, solid target could be irradiated with relatively low-energy (0.8-3.2 MeV) deuterons to produce [^{13}N]NH_3 by the ^{12}C(d,n)^{13}N reaction. This was accomplished by heating a graphite target in a stream of pure oxygen at 800°C, and $^{13}NO_2$– (99% radioactivity produced) was eluted with water and converted to [^{13}N]NH_3 with Raney nickel. The total extraction, trapping, and synthesis time was <17 min with a radiochemical purity of nearly 100%.

Mulholland et al. (22) reported a method of direct simultaneous production of [^{13}N]NH_3 and [^{15}O]H_2O with the use of 26 MeV proton irradiation and a double liquid chamber. Suzuki et al. (23) designed an automated system that used10 mM ethanol solution saturated with pure O_2 gas as the target and bombardedment with 18 MeV protons. Krasikova et al. (24) reported an alternative method that used low-pressure methane gas (150-550 kPa) in the natural water target irradiated with protons. The radiochemical purity of [^{13}N]NH_3 was >99% even at very high beam currents. Firouzbakht et al. (25) used a cryogenic target containing frozen water for the ^{16}O(p,α)^{13}N reaction, and they found that this procedure (with beam currents from 1 μA to 20 μA) could produce [^{13}N]NH_3 directly because low temperature decreased radiolysis. The radiochemical purity of the [^{13}N]NH_3 produced was >95%. When frozen carbon dioxide was irradiated, >95% of ^{13}N activity was in the form of nitrate and nitrite.

In Vitro Studies: Testing in Cells and Tissues

[PubMed]

Isolated arterially perfused rabbit interventricular septa (n = 9 at 28°C, n = 10 at 37°C) were used to study the relationship between blood flow, myocardial uptake, and the metabolism and clearance of [^{13}N]NH_3 (8). Analysis of the time-activity curves revealed that the [^{13}N]NH_3 kinetics were best described by three components. Component 1, with a short clearance $t_{½}$ of <7 min, was consistent with a freely diffusible NH_3 compartment. A large metabolic compartment was primarily responsible for component 3, which had a long clearance $t_{½}$ of 30 to 500 min. At 37°C and 15 min after injection, all radioactivity was essentially in component 3. In another study, glutamine synthetase appeared to be responsible for retention of [^{13}N]NH_3 radioactivity in rabbit myocardium (26). In their study of [^{13}N]NH_3 uptake in myocardial single cells, Rauch et al. (27) found that in addition to metabolic trapping, the extraction of [^{13}N]NH_3 might also be influenced by cell membrane integrity, intracellular-extracellular pH gradient, and possibly an anion exchange system for bicarbonate.

Animal Studies

Rodents

[PubMed]

Imaging studies with [^{13}N]NH_3 in mice showed activity localization in the liver, myocardium, and bladder (12). The radioactivity cleared from the blood very rapidly with 85% clearance in the first minute, and 4.7% of the injected dose (ID) was excreted by the kidneys in 35 min. The biodistribution of [^{13}N]NH_3 was studied in rats (28). The rats were euthanized at different time intervals between 0.2 and 50 min after i.v. injection of 18.5 MBq (0.5 mCi)/kg of [^{13}N]NH_3 with an estimated specific activity of 74 × 10^5 to 148 × 10^5 GBq/mol (2 × 10^5 to 4 × 10^5 Ci/mol) at the EOB. The highest initial whole-organ radioactivities at 0.2 min after injection were in the lungs (20.1 ± 2.9% ID n = 5), kidneys (13.6 ± 1.2% ID), and heart (2.6 ± 0.18% ID), and at 50 min these values decreased to 1.51 ± 0.17% ID, 1.82 ± 0.22% ID, and 0.92 ± 0.06% ID, respectively. The radioactivity in the liver was 4.83 ± 0.73% ID at 0.2 min and then increased to a maximum of 14.4 ± 0.7% ID at 20 min. The radioactivity in the brain was 0.55 ± 0.04% ID at 0.2 min and then increased to a maximum of 0.89 ± 0.1% ID at 10 min.

Cooper et al. (29) studied the cerebral uptake and metabolism of [^{13}N]NH_3 in conscious rats, and they found that [^{13}N]NH_3 entered the brain from the blood largely by diffusion. This and other studies (30) indicated that the major route for metabolism of [^{13}N]NH_3 in the brain was incorporation into [amide-^{13}N]glutamine. Lockwood et al. (31) showed that the brain-blood pH gradient had a major influence on the uptake of [^{13}N]NH_3 by the brain.

Other Non-Primate Mammals

[PubMed]

The localization of [^{13}N]NH_3 was studied in normal dogs by three methods of administration (inhalation, i.v., and s.c.) (4). All three methods showed similar imaging results. The radioactivity localization was mainly in the brain, heart, liver, and bladder. Approximately 10-20% of the ID was cleared rapidly from the blood by the kidneys and collected in the urinary bladder. The clearance $t_{½}$ of the kidneys was 7.7 to 10.6 min. In a dog study, Carter et al. (32) showed that increased blood pH increased brain uptake of [^{13}N]NH_3 and decreased blood pH decreased liver uptake of [^{13}N]NH_3. Rosenspire et al. (33) studied the metabolic fate of [^{13}N]NH_3 in dogs, and they found that urea was the predominant metabolite. Neutral amino acids (i.e., glutamine and asparagine) were the second most predominant metabolites. Schelbert et al. (34, 35) found a relatively linear relationship between myocardial blood flow (from 0 to 500 ml/min/100 g in dogs) and myocardial [^{13}N]NH_3 radioactivity concentration. In comparison, the human physiologic range was from 0 to 350 ml/min/100 g. Other studies in dogs (36, 37) indicated that [^{13}N]NH_3 provided qualitative and quantitative information of myocardial blood flow comparable to data measured by microspheres and [^{15}O]H_2O.

The uptake kinetics of [^{13}N]NH_3 in the liver were studied in a pig model (38). A simplified circulatory model was proposed to estimate the hepatic clearance of [^{13}N]NH_3. The hepatic clearance was estimated to be 10.25 ± 1.84 ml/min/kg (n = 4).

Non-Human Primates

[PubMed]

The movement of [^{13}N]NH_3 from blood to brain was studied in rhesus monkeys (39). A regional residue detection model was proposed for the cerebral blood flow. The data revealed a diffusion limitation for the transport of [^{13}N]NH_3 from blood to brain because of the low permeability of [^{13}N]NH_4^+.Therefore at high flow rates the brain uptake of [^{13}N]NH_3 was no longer linear with flow increases.

Human Studies

[PubMed]

Harper et al. (12) performed imaging with 370 MBq (10 mCi) at the time of administration, (TOA) of [^{13}N]NH_3 in 2 healthy volunteers and showed that radioactivity localized in the myocardium, mediastinum, and liver. There was an initial moderate uptake in the lungs, and it was washed out after 5-10 min. In a metabolic study (33), 9 healthy male volunteers received iv. administration of 740 MBq (20 mCi at the TOA) of [^{13}N]NH_3 in normal saline. About 93.1 ± 4.9% (n = 6) of the blood radioactivity remained as [^{13}N]NH_3 within the first 2 min but was decreased to 50.2 ± 18.9% (n = 5) at 5 min after injection. At 1 min, the blood radioactivities associated with [^{13}N]glutamine and [^{13}N]urea were 3.0 ± 2.4% (n = 6) and 3.1 ± 4.6%, respectively. By 5 min, the radioactivities for [^{13}N]glutamine and [^{13}N]urea had increased to 16.2 ± 11.2% (n = 5) and 32.7 ± 10.0%, respectively. Lockwood et al. (11) reported a study of [^{13}N]NH_3 metabolism in 5 normal subjects with a dose of 370 MBq (10 mCi at the TOA) that showed that the rates of both radioactivity clearance from the vascular compartment and brain ammonia utilization were linear functions of its arterial concentration. About 47 ± 3% of [^{13}N]NH_3 radioactivity was taken up by the brain during a single pass from the arterial blood, and 7.4 ± 0.3% of [^{13}N]NH_3 was metabolized by the brain. Approximately 50% of the arterial [^{13}N]NH_3 was metabolized by the skeletal muscle. Changes in [^{13}N]NH_3 kinetics were reported in patients with tumors, hypopituitarism, and liver diseases [PubMed].

In 1980, Lockwood (40) reported the radiation absorbed doses of i.v. injection of [^{13}N]NH_3 with the use of body distribution data and the MIRD model. The urinary bladder wall was the critical organ with the highest total absorbed dose (0.014 mGy/MBq or 51 mrad/mCi). The whole body, liver, red marrow, ovaries, and testes received 0.0015 mGy/MBq (5.5 mrad/mCi), 0.0046 mGy/MBq (17 mrad/mCi), 0.0015 mGy/MBq (5.4 mrad/mCi), 0.0027 mGy/MBq (9.8 mrad/mCi), and 0.00027 mGy/Bq (1 mrad/mCi), respectively. The brain to brain-absorbed dose was 0.0043 mGy/MBq (16 mrad/mCi). Complete radiation dosimetry of [^{13}N]NH_3 for adults has also been tabulated.

Hickey et al. (41) in a 2005 study compared the measurement of myocardial perfusion using [^{13}N]NH_3 with that of [^{15}O]H_2O in healthy volunteers, and they found that there was a discrepancy between the two measurements in a 2-compartment model analysis. The underestimation by [^{13}N]NH_3 was most likely attributable to the regional myocardial uptake variation and metabolism of [^{13}N]NH_3. This could be minimized by use of a 3-compartment model for data analysis. Other studies [PubMed] have shown the clinical utility of [^{13}N]NH_3 for quantification of myocardial blood flow in humans. In a study of 27 patients, Khorsand et al. (42) reported that gated cardiac [^{13}N]NH_3 imaging could be used for the estimation of LV function. In a study of 21 patients admitted for the assessment of myocardial perfusion with dynamic [^{13}N]NH_3 PET, the absolute quantification of myocardial blood flow with 3-dimensional PET appeared to be in excellent agreement with those obtained with the 2-dimensional technique (43).

Supplemental Information

[Disclaimers]

Draft of Review and Evaluation of Pharmacology and Toxicology Data

Medical and Statistical Review

NIH Support

NIH HL-27841-01-03; NCI CA-18153-03, CA-08748-14; USPHS AM-16739, NS-00343; NIH DK-16739; NINCDS NS-05820, NS15665; NIH HL-11351-13, HL-27841-01; NCI 08748-11B; NIH RO1 HL-41047-01; USPHS GM-14889-06, 1 F11 NB-2169-01; NIH HL-29845, HL-33177, HL-29845-01; USPHS HE-06664, HL-15860, GM-16712, HV-71443; NCI CA-08748; NIH HL-43884; NINDS NS-15380; PHS NINCDS NS-15380; USPHS P01 HL-13851-11; NIH IR43HL48969, 2R44CA53953; NIH NS15655; NIH NS-02149; USPHS 1 P01 GM-18940-01, 43-NHL1-68-1334; NINCDS NS-05820, NS-14996, NIH 89-2359Ja, HL-27555, NIH HL-29845, HL-33177.

References

1. Clark, J.C., F.I. Aigbirdhio, Chemistry of nitrogen-13 and oxygen-15, in Handbook of Radiopharmaceuticals, M.J. Welch, C.S. Redvanly, Editor. 2003, John Wiley & Sons Inc.: Chichester, West Sussex, England. p. 119-140.
2. Phelps M.E., Hoffman E.J., Raybaud C. Factors which affect cerebral uptake and retention of 13NH3. Stroke. 1977;**8**(6):694–702. PubMed PMID: 22147.
3. Schelbert, H.R., PET studies of the heart., in Positron Emission Tomography and Autoradiography, M.E. Phelps, J.C. Mazziota and H.R. Schelbert, Editor. 1986, Raven Press: New York. p. 581-662.
4. Monahan W.G., Tilbury R.S., Laughlin J.S. Uptake of 13 N-labeled ammonia. J Nucl Med. 1972;**13**(4):274–7. PubMed PMID: 5011778.
5. Mudge, G.H., Agents affecting volume and composition of body fluids, in Goodman and Gilman's the pharmacological basis of therapeutics, A.G. Gilman, L.S. Goodman and A. Gilman, Editor. 1980, MacMillan Publishing Co., Inc.: New York. p. 869-870.
6. Walsh W.F., Fill H.R., Harper P.V. Nitrogen-13-labeled ammonia for myocardial imaging. Semin Nucl Med. 1977;**7**(1):59–66. PubMed PMID: 835025.
7. Straatmann M.G. A look at 13N and 15O in radiopharmaceuticals. Int J Appl Radiat Isot. 1977;**28**(1-2):13–20. PubMed PMID: 323156.
8. Krivokapich J., Huang S.C., Phelps M.E., MacDonald N.S., Shine K.I. Dependence of 13NH3 myocardial extraction and clearance on flow and metabolism. Am J Physiol. 1982;**242**(4):H536–42. PubMed PMID: 7065268.
9. Schelstraete K., Simons M., Deman J., Vermeulen F.L., Slegers G., Vandecasteele C., Goethals P., De Schryver A. Uptake of 13N-ammonia by human tumours as studied by positron emission tomography. Br J Radiol. 1982;**55**(659):797–804. PubMed PMID: 6982741.
10. Joliot F., Curie I. Artifical production of a new kind of radio-element. Nature. 1934;**133**:201–202.

11. Lockwood A.H., McDonald J.M., Reiman R.E., Gelbard A.S., Laughlin J.S., Duffy T.E., Plum F. The dynamics of ammonia metabolism in man. Effects of liver disease and hyperammonemia. J Clin Invest. 1979;**63**(3):449–60. PubMed PMID: 429564.
12. Harper P.V., Lathrop K.A., Krizek H., Lembares N., Stark V., Hoffer P.B. Clinical feasibility of myocardial imaging with 13 NH 3. J Nucl Med. 1972;**13**(4):278–80. PubMed PMID: 5011779.
13. van den Heuvel A.F., Blanksma P.K., Siebelink H.M., van Wijk L.M., Boomsma F., Vaalburg W., Crijns H.J., van Veldhuisen D.J. Impairment of myocardial blood flow reserve in patients with asymptomatic left ventricular dysfunction: effects of ACE-inhibition with perindopril. Int J Cardiovasc Imaging. 2001;**17**(5):353–9. PubMed PMID: 12025949.
14. Ido T., Iwata R. Fully automated synthesis of 13NH3. Journal of Labelled Compounds and Radiopharmaceuticals. 1981;**XVIII**(1-2):244–246.
15. Wieland B., Bida G., Padgett H., Hendry G., Zippi E., Kabalka G., Morelle J.L., Verbruggen R., Ghyoot M. In-target production of [13N]ammonia via proton irradiation of dilute aqueous ethanol and acetic acid mixtures. Int J Rad Appl Instrum [A]. 1991;**42**(11):1095–8. PubMed PMID: 1667316.
16. Berridge M.S., Landmeier B.J. In-target production of [13N]ammonia: target design, products, and operating parameters. Appl Radiat Isot. 1993;**44**(12):1433–41. PubMed PMID: 8257962.
17. Ferrieri R.A., Schlyer D.J., Wieland B.W., Wolf A.P. On-line production of 13N-nitrogen gas from a solid enriched 13C-target and its application to 13N-ammonia synthesis using microwave radiation. Int. J. Appl. Radiat. Isot. 1983;**34**(6):897–900.
18. Bida G., Wieland B. W., Ruth T.J., Schmidt D.G., Hendry G.O., Keen R.E. An economical target for nitrogen-13 production by proton bombardment of a slurry of C-13 powder in O-16 water. J. Labelled Compd. Radiopharm. 1986;**23**:1217–1218.
19. Welch M.J., Lifton J.F. The fate of nitrogen-13 formed by the 12C(d,n)13N reaction in inorganic carbides. Journal of the American Chemical Society. 1971;**93**(14):3385–3388.
20. Shefer R.E., Hughey B.J., Klinkowstein R.E., Welch M.J., Dence C.S. A windowless 13N production target for use with low energy deuteron accelerators. Nucl Med Biol. 1994;**21**(7):977–86. PubMed PMID: 9234353.
21. Dence C.S., Welch M.J., Hughey B.J., Shefer R.E., Klinkowstein R.E. Production of [13N]ammonia applicable to low energy accelerators. Nucl Med Biol. 1994;**21**(7):987–96. PubMed PMID: 9234354.
22. Mulholland G.K., Kilbourn M.R., Moskwa J.J. Direct simultaneous production of [15O]water and [13N]ammonia or [18F]fluoride ion by 26 MeV proton irradiation of a double chamber water target. Int J Rad Appl Instrum [A]. 1990;**41**(12):1193–9. PubMed PMID: 1963419.
23. Suzuki K., Yoshida Y., Shikano N., Kubodera A. and Development of an automated system for the quick production of 13N-labeled compounds with high specific activity using anhydrous [13N]NH3. Applied Radiation adn Isotopes, 50: p. 1033-1038. 1999.

24. Krasikova R.N., Fedorova O.S., Korsakov M.V., Bennington B.I., Berridge M.S. Improved [N-13]ammonia yield from the proton irradiation of water using methane gas. Appl. Radiat. Isot. 1999;**51**:395–401.
25. Firouzbakht M.L., Schlyer D.J., Wolf A.P., Fowler J.S. Mechanism of nitrogen-13-labeled ammonia formation in a cryogenic water target. Nucl Med Biol. 1999;**26**(4):437–41. PubMed PMID: 10382848.
26. Krivokapich J., Barrio J.R., Phelps M.E., Watanabe C.R., Keen R.E., Padgett H.C., Douglas A., Shine K.I. Kinetic characterization of 13NH3 and [13N]glutamine metabolism in rabbit heart. Am J Physiol. 1984;**246**(2 Pt 2):H267–73. PubMed PMID: 6696136.
27. Rauch B., Helus F., Grunze M., Braunwell E., Mall G., Hasselbach W., Kubler W. Kinetics of 13N-ammonia uptake in myocardial single cells indicating potential limitations in its applicability as a marker of myocardial blood flow. Circulation. 1985;**71**(2):387–93. PubMed PMID: 3965179.
28. Freed B.R., McQuinn R.L., Tilbury R.S., Digenis G.A. Distribution of 13N in rat tissues following intravenous administration of nitroso-labeled BCNU. Cancer Chemother Pharmacol. 1982;**10**(1):16–21. PubMed PMID: 7160041.
29. Cooper A.J., McDonald J.M., Gelbard A.S., Gledhill R.F., Duffy T.E. The metabolic fate of 13N-labeled ammonia in rat brain. J Biol Chem. 1979;**254**(12):4982–92. PubMed PMID: 36379.
30. Cooper A.J., Lai J.C. Cerebral ammonia metabolism in normal and hyperammonemic rats. Neurochem Pathol. 1987;**6**(1-2):67–95. PubMed PMID: 2888066.
31. Lockwood A.H., Finn R.D., Campbell J.A., Richman T.B. Factors that affect the uptake of ammonia by the brain: the blood-brain pH gradient. Brain Res. 1980;**181**(2):259–66. PubMed PMID: 7350966.
32. Carter C.C., Lifton J.F., Welch M.J. Organ uptake and blood pH and concentration effects of ammonia in dogs determined with ammonia labeled with 10 minute half-lived nitrogen 13. Neurology. 1973;**23**(2):204–13. PubMed PMID: 4734515.
33. Rosenspire K.C., Schwaiger M., Mangner T.J., Hutchins G.D., Sutorik A., Kuhl D.E. Metabolic fate of [13N]ammonia in human and canine blood. J Nucl Med. 1990;**31**(2):163–7. PubMed PMID: 2313355.
34. Schelbert H.R., Phelps M.E., Hoffman E.J., Huang S.C., Selin C.E., Kuhl D.E. Regional myocardial perfusion assessed with N-13 labeled ammonia and positron emission computerized axial tomography. Am J Cardiol. 1979;**43**(2):209–18. PubMed PMID: 760475.
35. Schelbert H.R., Phelps M.E., Huang S.C., MacDonald N.S., Hansen H., Selin C., Kuhl D.E. N-13 ammonia as an indicator of myocardial blood flow. Circulation. 1981;**63**(6):1259–72. PubMed PMID: 7226473.
36. Muzik O., Duvernoy C., Beanlands R.S., Sawada S., Dayanikli F., Wolfe E.R., Schwaiger M. Assessment of diagnostic performance of quantitative flow measurements in normal subjects and patients with angiographically documented coronary artery disease by means of nitrogen-13 ammonia and positron emission tomography. J Am Coll Cardiol. 1998;**31**(3):534–40. PubMed PMID: 9502631.

37. Bol A., Melin J.A., Vanoverschelde J.L., Baudhuin T., Vogelaers D., De Pauw M., Michel C., Luxen A., Labar D., Cogneau M., Robert A., Heyndrickx G., Wijns W. Direct comparison of [13N]ammonia and [15O]water estimates of perfusion with quantification of regional myocardial blood flow by microspheres. Circulation. 1993;**87**(2):512–25. PubMed PMID: 8425298.
38. Weiss M., Roelsgaard K., Bender D., Keiding S. Determinants of [13N]ammonia kinetics in hepatic PET experiments: a minimal recirculatory model. Eur J Nucl Med Mol Imaging. 2002;**29**(12):1648–56. PubMed PMID: 12458400.
39. Raichle M.E., Larson K.B. The significance of the NH3-NH+(4) equilibrium on the passage of 13N-ammonia from blood to brain. A new regional residue detection model. Circ Res. 1981;**48**(6 Pt 1):913–37. PubMed PMID: 7226451.
40. Lockwood A.H. Absorbed doses of radiation after an intravenous injection of N-13 ammonia in man: concise communication. J Nucl Med. 1980;**21**(3):276–8. PubMed PMID: 7365520.
41. Hickey K.T., Sciacca R.R., Chou R.L., Rodriguez O., Bokhari S., Bergmann S.R. An improved model for the measurement of myocardial perfusion in human beings using N-13 ammonia. J Nucl Cardiol. 2005;**12**(3):311–7. PubMed PMID: 15944536.
42. Khorsand A., Graf S., Eidherr H., Wadsak W., Kletter K., Sochor H., Schuster E., Porenta G. Gated Cardiac 13N-NH3 PET for Assessment of Left Ventricular Volumes, Mass, and Ejection Fraction: Comparison with Electrocardiography-Gated 18F-FDG PET. J Nucl Med. 2005;**46**(12):2009–13. PubMed PMID: 16330564.
43. Schepis T., Gaemperli O., Treyer V., Valenta I., Burger C., Koepfli P., Namdar M., Adachi I., Alkadhi H., Kaufmann P.A. Absolute quantification of myocardial blood flow with 13N-ammonia and 3-dimensional PET. J Nucl Med. 2007;**48**(11):1783–9. PubMed PMID: 17942816.